JOURNAL OF MULTIFUNCTIONAL MATERIALS & PHOTOSCIENCE
6(1), June 2015, pp. 27-35

Preparation of Microcrystalline $PbMoO_4$: Er^{3+}/Yb^{3+} Phosphors by Microwave Sol-Gel Method and their Upconversion Photoluminescence Properties

Chang Sung Lim

Department of Advanced Materials Science & Engineering, Hanseo University, Seosan 356-706 Republic of Korea

Abstract: Microcrystalline $Pb_{1-x}MoO_4$:Er^{3+}/Yb^{3+} phosphors with doping concentrations of Er^{3+} and Yb^{3+} (x = Er^{3+} + Yb^{3+}, Er^{3+} = 0.05, 0.1, 0.2 and Yb^{3+}= 0.2, 0.45) were successfully prepared by microwave sol-gel method, and their upconversion photoluminescence properties were investigated. Well-crystallized particles, formed after heat-treatment at 900°C for 16 h, showed a fine and homogeneous morphology with particle sizes of 2-5 μm. Under excitation at 980 nm, $Pb_{0.7}MoO_4$: $Er_{0.1}Yb_{0.2}$ and $Pb_{0.5}MoO_4$: $Er_{0.05}Yb_{0.45}$ particles exhibited a strong 525-nm emission band, a weak 550-nm emission band in the green region, and a very weak 655-nm emission band in the red region. The Raman spectra of the doped particles indicated the presence of strong peaks at higher and lower frequencies induced by disorderd structures of $Pb_{1-x}MoO_4$ by the incorporation of the Er^{3+} and Yb^{3+} ions into the crystal lattice, which resulted in the unit cell shrinkage accompanying the highly modulated structure.

***Key words*:** $Pb_{1-x}MoO_4$:Er^{3+}/Yb^{3+} phosphors, Microwave sol-gel, Upconversion luminescence Raman spectroscopy.

Introduction

Rare earth doped upconversion (UC) phosphors have attracted great attention because of the conversion from near infrared radiation of low energy to visible radiation of high energy. These UC photoluminescence particles have potential applications in various fields, including biomedical imaging, owing to their unique UC optical behaviors that offer improved light penetration depth, high chemical and photo stability, the absence of auto-fluorescence during imaging, sharp emission bands, and high resistance to photobleaching. These properties overcome many of the current limitations in traditional photoluminescence materials [1-3]. It is possible for the structure of the molybdate compounds to be transformed to a highly disordered tetragonal scheelite structure from the monoclinic structure. It is possible for the trivalent rare earth ions in the disordered tetragonal-phase to be partially substituted by Er^{3+} and Yb^{3+} ions, these ions are effectively

Corresponding author: cslim@hanseo.ac.kr*

doped into the crystal lattices of the tetragonal phase due to the similar radii of the trivalent rare earth ions, this results in the excellent UC photoluminescence properties [4-6]. Among rare earth ions, the Er^{3+} ion is suitable for converting infrared to visible light through the UC process due to its appropriate electronic energy level configuration. The co-doped Yb^{3+} ion and Er^{3+} ion can remarkably enhance the UC efficiency for the shift from infrared to visible light due to the efficiency of the energy transfer from Yb^{3+} to Er^{3+}. The Yb^{3+} ion, as a sensitizer, can be effectively excited by an incident light source energy. This energy is transferred to the activator from which radiation can be emitted. The Er^{3+} ion activator is the luminescence center of the UC particles, while the sensitizer enhances the UC luminescence efficiency [7-9].

Recently, rare earth activated molybdates have attracted great attention because of their spectroscopic characteristics and excellent upconversion photoluminescence properties. Several processes have been developed via specific preparation processes, including solid-state reactions [9-14], co-precipitation [15, 16], the sol-gel method [4-7], the hydrothermal method [17, 18], the Pechini method [19, 20], organic gel-thermal decomposition [21], and the microwave-assisted hydrothermal method [22]. For practical application of UC photoluminescence in products such as lasers, three-dimensional displays, light-emitting devices, and biological detectors, features such as the homogeneous UC particle size distribution and morphology need to be well defined. Usually, molybdates are prepared by a solid-state method that requires high temperatures, a lengthy heating process and subsequent grinding, this results in a loss of the emission intensity and an increase in cost. The sol-gel process provides some advantages over the conventional solid-state method, including good homogeneity, low calcination temperature, small particle size and narrow particle size distribution optimal for good luminescent characteristics. However, the sol-gel process has a disadvantage in that it takes a long time for gelation. Compared with the usual methods, microwave synthesis has the advantages of a very short reaction time, small-size particles, narrow particle size distribution, and high purity of final polycrystalline samples. Microwave heating is delivered to the material surface by radiant and/or convection heating, which is transferred to the bulk of the material via conduction [23, 24]. Microwave sol-gel process is a cost-effective method that provides high homogeneity and is easy to scale-up, and it is emerging as a viable alternative approach for the quick synthesis of high-quality luminescent materials.

In this study, $Pb_{1-x}MoO_4$: Er^{3+}/Yb^{3+} phosphors with doping concentrations of Er^{3+} and Yb^{3+} ($x = Er^{3+} + Yb^{3+}$, $Er^{3+} = 0.05, 0.1, 0.2$ and $Yb^{3+} = 0.2, 0.45$) phosphors were prepared by the microwave sol-gel method, followed by heat treatment. The synthesized particles were characterized by X-ray diffraction (XRD), scanning electron microscopy (SEM), and energy-dispersive X-ray spectroscopy (EDS). The optical properties were examined comparatively using photoluminescence (PL) emission and Raman spectroscopy.

Experimental

Appropriate stoichiometric amounts of $Pb(NO_3)_2$ (99%, Sigma-Aldrich, USA), $(NH_4)_6Mo_7O_{24}\cdot 4H_2O$ (99%, Alfa Aesar, USA), $Er(NO_3)_3\cdot 5H_2O$ (99.9%, Sigma-Aldrich, USA),

$Yb(NO_3)_3 \cdot 5H_2O$ (99.9%, Sigma-Aldrich, USA), citric acid (99.5%, Daejung Chemicals, Korea), NH_4OH (A.R.), ethylene glycol (A.R.) and distilled water were used to prepare $PbMoO_4$, $Pb_{0.8}MoO_4:Er_{0.2}$, $Pb_{0.7}MoO_4:Er_{0.1}Yb_{0.2}$ and $Pb_{0.5}MoO_4:Er_{0.05}Yb_{0.45}$ compounds with doping concentrations of Er^{3+} and Yb^{3+} (Er^{3+} = 0.05, 0.1, 0.2 and Yb^{3+}= 0.2, 0.45). To prepare $PbMoO_4$, 0.4 mol% $Pb(NO_3)_2$ and 0.14 mol% $(NH_4)_6Mo_7O_{24} \cdot 4H_2O$ were dissolved in 20 mL of ethylene glycol and 80 mL of 5M NH_4OH under vigorous stirring and heating. Subsequently, citric acid (with a molar ratio of citric acid to total metal ions of 2:1) was dissolved in 100 mL of distilled water under vigorous stirring and heating. Then, the solutions were mixed together under vigorous stirring and heating at 80-100°C. Finally, highly transparent solutions were obtained and adjusted to pH=7-8 by the addition of NH_4OH or citric acid. In order to prepare $Pb_{0.8}MoO_4:Er_{0.2}$, the mixture of 0.32 mol% $Pb(NO_3)_2$ with 0.08 mol% $Er(NO_3)_3 \cdot 5H_2O$ was used for the creation of the rare earth solution. In order to prepare $Pb_{0.7}MoO_4:Er_{0.1}Yb_{0.2}$, the mixture of 0.28 mol% $Pb(NO_3)_2$ with 0.04 mol% $Er(NO_3)_3 \cdot 5H_2O$ and 0.08 mol% $Yb(NO_3)_3 \cdot 5H_2O$ was used for the creation of the rare earth solution. In order to prepare $Pb_{0.5}MoO_4:Er_{0.05}Yb_{0.45}$, the rare earth containing solution was generated using 0.2 mol% $Pb(NO_3)_2$ with 0.02 mol% $Er(NO_3)_3 \cdot 5H_2O$ and 0.18 mol% $Yb(NO_3)_3 \cdot 5H_2O$.

The transparent solutions were placed for 30 min into a microwave oven operating at a frequency of 2.45 GHz with a maximum output-power of 1250 W. The working cycle of the microwave reaction was controlled very precisely using a regime of 40 s on and 20 s off for 15 min, followed by further treatment of 30 s on and 30 s off for 15 min. The ethylene glycol was evaporated slowly at its boiling point. Ethylene glycol is a polar solvent at its boiling point of 197°C, this solvent is a good candidate for the microwave process. If ethylene glycol is used as the solvent, the reactions proceed at the boiling point temperature. When microwave radiation is supplied to the ethylene-glycol-based solution, the components dissolved in the ethylene glycol can couple. The charged particles vibrate in the electric field interdependently when a large amount of microwave radiation is supplied to the ethylene glycol. The samples were treated with ultrasonic radiation for 10 min to produce a light yellow transparent sol. After this, the light yellow transparent sols were dried at 120°C in a dry oven to obtain black dried gels. The black dried gels were ground and heat-treated at 900°C for 16 h with 100°C intervals between 600-900°C. Finally, white particles were obtained for the pure $PbMoO_4$ and pink particles were obtained for the doped compositions.

The phase composition of the synthesized particles was identified using XRD (D/MAX 2200, Rigaku, Japan). The microstructure and surface morphology of the synthesized particles were observed using SEM/EDS (JSM-5600, JEOL, Japan). The PL spectra were recorded using a spectrophotometer (Perkin Elmer LS55, UK) at room temperature. Raman spectroscopy measurements were performed using a LabRam Aramis (Horiba Jobin-Yvon, France). The 514.5-nm line of an Ar ion laser was used as the excitation source; the power on the samples was kept at 0.5 mW.

Results and Discussion

Fig. 1 shows the XRD patterns of the (a) JCPDS 44-1486 data of $PbMoO_4$, and the synthesized (b) $PbMoO_4$, (c) $Pb_{0.8}MoO_4:Er_{0.2}$, (d) $Pb_{0.7}MoO_4:Er_{0.1}Yb_{0.2}$, and (e) $Pb_{0.5}MoO_4:Er_{0.05}Yb_{0.45}$

particles. The crystal structures are in good agreement with the crystallographic data of $PbMoO_4$ (JCPDS 44-1486). The pure (b) $PbMoO_4$ and (c) $Pb_{0.8}MoO_4$:$Er_{0.2}$ have no impurity phases. Impurity phases were detected at18.5°, 25° and 31° in Fig. 1(d), and 18.5°, 25°, 26°, 31°, 34°, 35° , 48°, 49°, and 49.5 as can be seen in Fig. 1(e). The foreign reflexes are marked with an asterisk in Fig. 1(e) when the doping concentration of Er^{3+}/Yb^{3+} is 0.02/0.18 mol%. A similar impurity phase was also observed in the case of Er^{3+}/Yb^{3+} doped $CaMoO_4$ phosphor when the doping concentration of Er^{3+}/Yb^{3+} is 0.02/0.18 mol% [25]. The foreign reflexes marked with an asterisk in Fig. 1(e) compared to the Er^{3+}/Yb^{3+} doped $CaMoO_4$ can be ascribed to the fact that Er^{3+} and Yb^{3+} ions are well substituted in the tetragonal-phase $PbMoO_4$: Er^{3+}/Yb^{3+} of the scheelite-type structure and form a new phase induced by the disorder of the $[MoO_4]^{2-}$ groups [25]. This suggests that the cyclic microwave-modified sol-gel route is suitable for the growth of $PbMoO_4$: Er^{3+}/Yb^{3+} crystallites. Post heat-treatment plays an important role in a well-defined crystallized morphology. To achieve a well-defined crystalline morphology of $PbMoO_4$, $Pb_{0.8}MoO_4$: $Er_{0.2}$, $Pb_{0.7}MoO_4$: $Er_{0.1}Yb_{0.2}$, and $Pb_{0.5}MoO_4$: $Er_{0.05}Yb_{0.45}$ phases need to be heat treated at 900°C for 16 h. It is assumed that the doping amount of Er^{3+}/Yb^{3+} has a great effect on the crystalline cell volume of the $PbMoO_4$, because of the different ionic sizes and energy band gaps. This means that the obtained samples possess a tetragonal-phase after partial substitution of

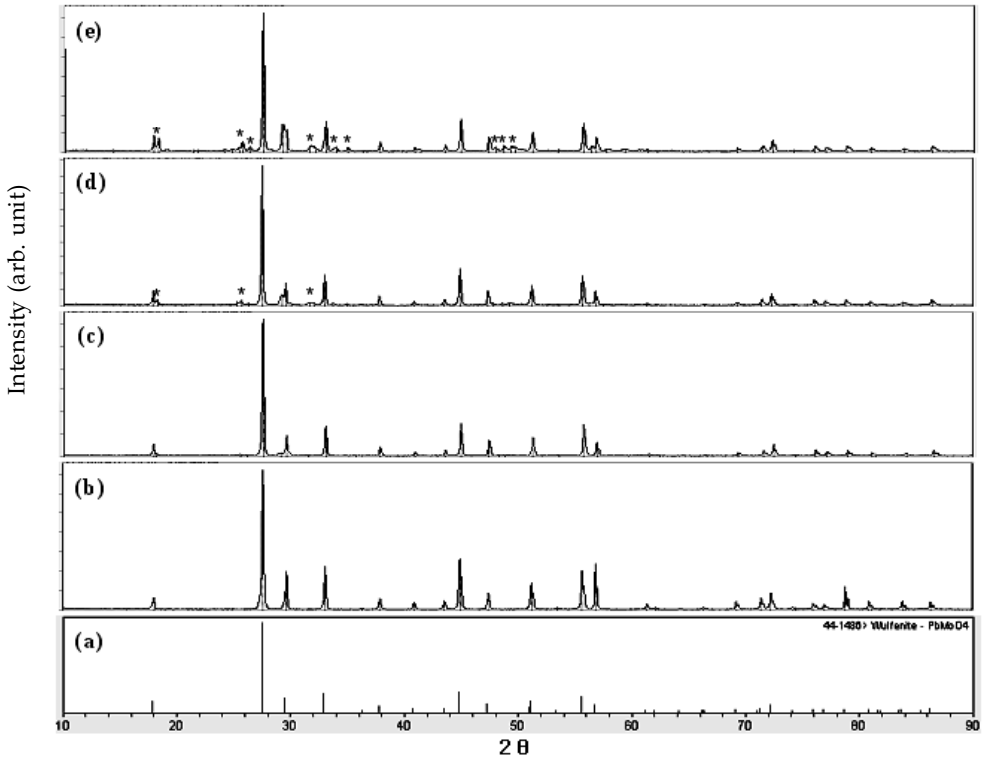

Figure 1: X-ray diffraction patterns of (a) JCPDS 44-1486 data of $PbMoO_4$, and the synthesized (b) $PbMoO_4$, (c) $Pb_{0.8}MoO_4$:$Er_{0.2}$, (d) $Pb_{0.7}MoO_4$:$Er_{0.1}Yb_{0.2}$, and (e) $Pb_{0.5}MoO_4$:$Er_{0.05}Yb_{0.45}$ particles

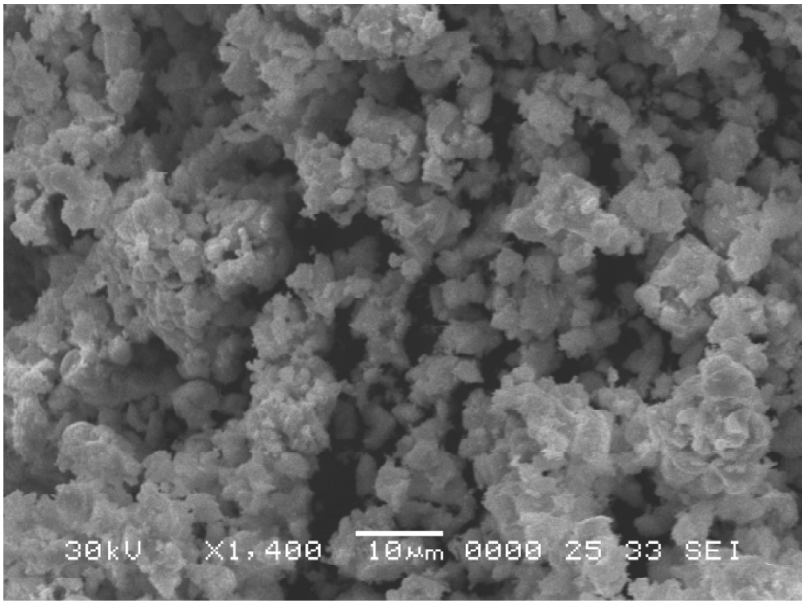

Figure 2: A scanning electron microscopy image of the $Pb_{0.5}MoO_4:Er_{0.05}Yb_{0.45}$ particles.

(a)

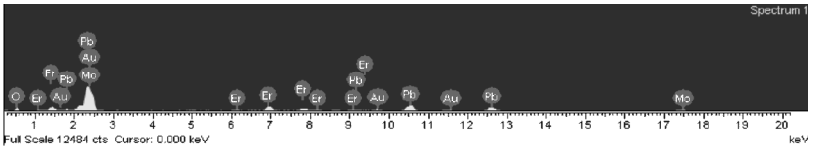

(b)

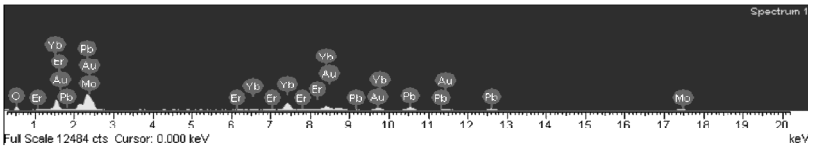

(c)

Spectrum	In stats.	O	Mo	Er	Pb	Total
Spectrum 1	Yes	20.98	25.07	22.26	31.69	100.00
Spectrum 2	Yes	20.17	25.01	22.25	32.57	100.00
Spectrum 3	Yes	20.33	23.56	23.11	33.00	100.00
Spectrum 4	Yes	20.25	23.45	23.21	33.09	100.00
Spectrum 5	Yes	23.31	23.48	21.49	31.72	100.00
Mean		21.01	24.11	22.47	32.41	100.00
Std. deviation		1.33	0.85	0.71	0.68	
Max.		23.31	25.07	23.21	33.09	
Min.		20.17	23.45	21.49	31.69	

(d)

Spectrum	In stats.	O	Mo	Er	Yb	Pb	Total
Spectrum 1	Yes	17.42	20.19	1.95	43.47	16.97	100.00
Spectrum 2	Yes	17.80	20.47	1.64	42.46	17.62	100.00
Spectrum 3	Yes	16.65	20.03	1.90	44.17	17.25	100.00
Spectrum 4	Yes	16.12	20.14	2.06	44.86	16.82	100.00
Mean		17.00	20.21	1.89	43.74	17.16	100.00
Std. deviation		0.76	0.19	0.17	1.02	0.35	
Max.		17.80	20.47	2.06	44.86	17.62	
Min.		16.12	20.03	1.64	42.46	16.82	

Figure 3: Energy-dispersive X-ray spectroscopy patterns of the synthesized (a) $Pb_{0.8}MoO_4:Er_{0.2}$ and (b) $Pb_{0.5}MoO_4:Er_{0.05}Yb_{0.45}$ particles, and quantitative compositions of (c) $Pb_{0.8}MoO_4:Er_{0.2}$ and (d) $Pb_{0.5}MoO_4:Er_{0.05}Yb_{0.45}$ particles.

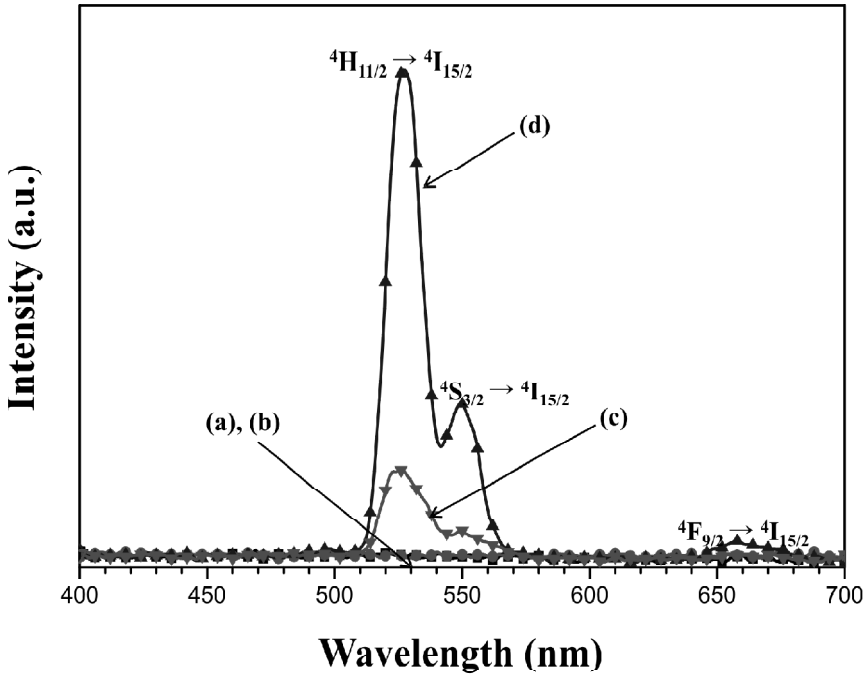

Figure 4: Upconversion photoluminescence emission spectra of (a) $PbMoO_4$, (b) $Pb_{0.8}MoO_4:Er_{0.2}$, (c) $Pb_{0.7}MoO_4:Er_{0.1}Yb_{0.2}$, and (d) $Pb_{0.5}MoO_4:Er_{0.05}Yb_{0.45}$ particles excited under 980 nm at room temperature.

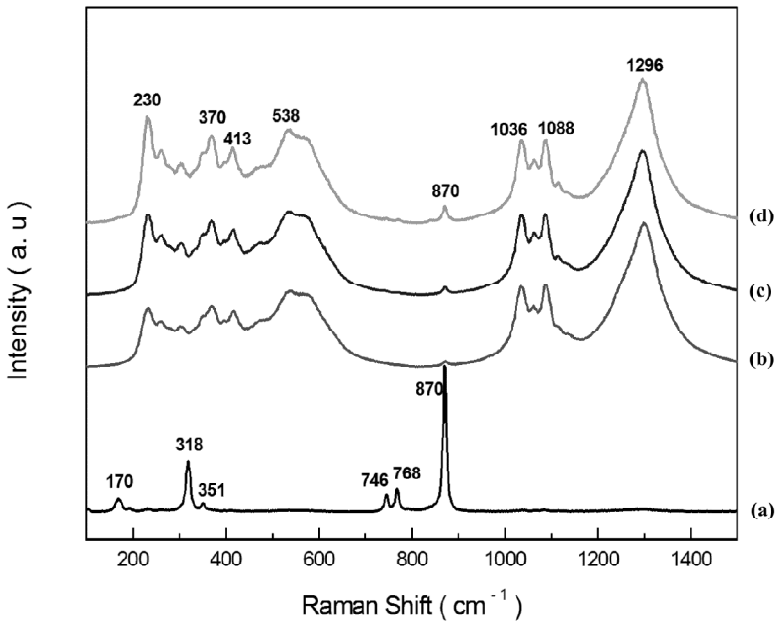

Figure 5: Raman spectra of the synthesized (a) $PbMoO_4$, (b) $Pb_{0.8}MoO_4:Er_{0.2}$, (c) $Pb_{0.7}MoO_4:Er_{0.1}Yb_{0.2}$, and (d) $Pb_{0.5}MoO_4:Er_{0.05}Yb_{0.45}$ .particles excited by the 514.5-nm line of an Ar ion laser at 0.5 mW.

Pb^{2+} by Er^{3+} and Yb^{3+} ions, and the ions are effectively doped into crystal lattices of the $PbMoO_4$ phase.

Fig. 2 shows a SEM image of the synthesized $Pb_{0.5}MoO_4$:$Er_{0.05}Yb_{0.45}$ particles. The as-synthesized samples are well crystallized with a fine and homogeneous morphology and particle size of 2-5 ìm. The sample has some agglomerated particles. It should be noted that the doping amounts for Er^{3+} and Yb^{3+} have a great effect on the morphological features.

Fig. 3 shows the energy-dispersive X-ray spectroscopy patterns of the synthesized (a) $Pb_{0.8}MoO_4$: $Er_{0.2}$ and (b) $Pb_{0.5}MoO_4$: $Er_{0.05}Yb_{0.45}$ particles; and the figures also shows the quantitative compositions of (c) $Pb_{0.8}MoO_4$: $Er_{0.2}$ and (d) $Pb_{0.5}MoO_4$: $Er_{0.05}Yb_{0.45}$ particles. The EDS pattern shows that the (a) $Pb_{0.8}MoO_4$: $Er_{0.2}$ and (b) $Pb_{0.5}MoO_4$: $Er_{0.05}Yb_{0.45}$ particles are composed of Pb, Mo, O and Er for the $Pb_{0.8}MoO_4$: $Er_{0.2}$ and of Pb, Mo, O, Er and Yb for the $Pb_{0.5}MoO_4$: $Er_{0.05}Yb_{0.45}$ particles. The quantitative compositions of (c) and (d) are in good relation with the nominal compositions of the particles. The relation of Pb, Mo, O, Er and Yb components shows that $Pb_{0.8}MoO_4$: $Er_{0.2}$ and $Pb_{0.5}MoO_4$: $Er_{0.05}Yb_{0.45}$ particles can be successfully synthesized using the cyclic microwave-modified sol-gel method. The cyclic microwave-modified sol-gel process of the moybdate provides the energy to synthesize the bulk of the material uniformly, so that fine particles with controlled morphology can be fabricated in a short time period.

Fig. 4 shows the UC photoluminescence emission spectra of the as-prepared (a) $PbMoO_4$, (b) $Pb_{0.8}MoO_4$: $Er_{0.2}$, (c) $Pb_{0.7}MoO_4$: $Er_{0.1}Yb_{0.2}$, and (d) $Pb_{0.5}MoO_4$: $Er_{0.05}Yb_{0.45}$ particles excited under 980 nm at room temperature. The UC intensities of (c) $Pb_{0.7}MoO_4$: $Er_{0.1}Yb_{0.2}$ and (d) $Pb_{0.5}MoO_4$: $Er_{0.05}Yb_{0.45}$ particles exhibited a strong 525-nm emission band, a weak 550-nm emission band in the green region and a very weak 655-nm emission band in the red region. The strong 525-nm emission band and the weak 550-nm emission band in the green region correspond to the $^2H_{11/2} \rightarrow {}^4I_{15/2}$ and $^4S_{3/2} \rightarrow {}^4I_{15/2}$ transitions, respectively, while the very weak emission 655-nm band in the red region corresponds to the $^4F_{9/2} \rightarrow {}^4I_{15/2}$ transition. The UC intensities of (a) $PbMoO_4$ and (b) $Pb_{0.8}MoO_4$:$Er_{0.2}$ particles were not detected. The UC intensity of (d) $Pb_{0.5}MoO_4$:$Er_{0.05}Yb_{0.45}$ is much higher than that of (c) $Pb_{0.7}MoO_4$: $Er_{0.1}Yb_{0.2}$. Similar results are also observed from Er^{3+}/Yb^{3+} co-doped in other host matrices, which are assigned to the UC emission spectra with the green emission intensity ($^2H_{11/2} \rightarrow {}^4I_{15/2}$ and $^4S_{3/2} \rightarrow {}^4I_{15/2}$ transitions) and the red emission intensity ($^4F_{9/2} \rightarrow {}^4I_{15/2}$ transition) [7, 10, 25-28]. The doping amounts of Er^{3+}/Yb^{3+} had a great effect on the morphological features of the particles and their UC fluorescence intensity. The Yb^{3+} ion sensitizer can be effectively excited by the energy of an incident light source, this energy is transferred to the activator where radiation can be emitted. The Er^{3+} ion activator is the luminescence center for these UC particles, and the sensitizer enhances the UC luminescence efficiency.

Fig. 5 shows the Raman spectra of the synthesized (a) $PbMoO_4$, (b) $Pb_{0.8}MoO_4$:$Er_{0.2}$, (c) $Pb_{0.7}MoO_4$:$Er_{0.1}Yb_{0.2}$, and (d) $Pb_{0.5}MoO_4$:$Er_{0.05}Yb_{0.45}$ particles excited by the 514.5-nm line of an Ar ion laser at 0.5 mW. The internal modes for the (a) $PbMoO_4$ particles were detected at 170, 318, 351, 746, 768 and 870 cm^{-1}, respectively. The well-resolved sharp peaks for the $PbMoO_4$ particles indicate a high crystallinity state of the synthesized particles. The internal

vibration mode frequencies are dependent on the lattice parameters and the degree of the partially covalent bond between the cation and molecular ionic group $[MoO_4]^{2-}$. The Raman spectra of (b) $Pb_{0.8}MoO_4:Er_{0.2}$, (c) $Pb_{0.7}MoO_4:Er_{0.1}Yb_{0.2}$, and (d) $Pb_{0.5}MoO_4:Er_{0.05}Yb_{0.45}$ particles indicate the very strong and dominant peaks at higher frequencies of 870, 1036, 1088 and 1296 cm^{-1} land and at lower frequencies of 230, 370, 413 and 538 cm^{-1}. The Raman spectra of the doped particles prove that the doping ions can influence the structure of the host materials. The combination of a heavy metal cation and the large inter-ionic distance for Er^{3+} and Yb^{3+} substitutions in Pb^{2+} sites in the lattice result in a low probability of UC and phonon-splitting relaxation in $Pb_{1-x}MoO_4$ crystals. It may be that these very strong and strange effects are generated by disorderd structures of $Pb_{1-x}MoO_4$ by the incorporation of the Er^{3+} and Yb^{3+} ions into the crystal lattice, which resulted in the unit cell shrinkage accompanying the highly modulated structure.

Conclusions

$Pb_{1-x}MoO_4$: Er^{3+}/Yb^{3+} phosphors with doping concentrations of Er^{3+} and Yb^{3+} (x = Er^{3+} + Yb^{3+}, Er^{3+} = 0.05, 0.1, 0.2 and Yb^{3+} = 0.2, 0.45) were successfully synthesized by the microwave sol-gel method. Well-crystallized particles formed after heat-treatment at 900°C for 16 h showed a fine and homogeneous morphology with particle sizes of 2-5 μm. Under excitation at 980 nm, the UC intensities of $Pb_{0.7}MoO_4$: $Er_{0.1}/Yb_{0.2}$ and $Pb_{0.5}MoO_4$: $Er_{0.05}/Yb_{0.45}$ particles exhibited a strong 525-nm emission band and a weak 550-nm emission band in the green region; these emissions were assigned to the $^2H_{11/2} \rightarrow {}^4I_{15/2}$ and $^4S_{3/2} \rightarrow {}^4I_{15/2}$ transitions, respectively, while a very weak 655-nm emission band in the red region was assigned to the $^4F_{9/2} \rightarrow {}^4I_{15/2}$ transition. The UC intensity of $Pb_{0.5}MoO_4$: $Er_{0.05}/Yb_{0.45}$ particles was much higher than that of the $Pb_{0.7}MoO_4:Er_{0.1}/Yb_{0.2}$ particles. The Raman spectra of the doped particles indicated the very strong and dominant peaks at higher frequencies of 870, 1036, 1088 and 1296 cm^{-1} land and at lower frequencies of 230, 370, 413 and 538 cm^{-1} induced by disorderd structures of $Pb_{1-x}MoO_4$ by the incorporation of the Er^{3+} and Yb^{3+} ions into the crystal lattice, which resulted in the unit cell shrinkage accompanying the highly modulated structure.

Acknowledgement

This study was supported by the Basic Science Research Program through the National Research Foundation of Korea (NRF), funded by the Ministry of Science, ICT & Future Planning (2014-046024).

References

[1] M. Wang, G. Abbineni, A. Clevenger, C. Mao, S. Xu, *Nanomedicine: Nanotech. Biology, and Medicine*, **7**, **710** (2011).

[2] A. Shalav, B.S. Richards, M.A. Green, *Sol. Ener. Mater. Sol. Cells*, **91**, 829 (2007).

[3] M. Lin, Y. Zho, S. Wang, M, Liu, Z. Duan, Y. Chen, F. Li, F. Xu, T. Lu, *Biol. Adv.*, **30**, 1551 (2012).

[4] J. Liao, D. Zhou, B. Yang, R. liu, Q. Zhang, Q. Zhou, *J. Lumin.*, **134**, 533 (2013).

[5] J. Sun, J. Xian, H. Du, *J. Phys. Chem. Solids*, **72**, 207 (2011).

[6] C. Guo, H. K. Yang, J.H. Jeong, *J. Lumin.*, **130**, 1390 (2010).

[7] J. Sun, J. Xian, H. Du, *J. Phys. Chem. Solids,* **72,** 207 (2011).

[8] V. K. Komarala, Y. Wang, M. Xiao, *Chem. Phys. Lett.,* **490,** 189 (2010).

[9] J. Sun, J. Xian, Z. Xia, H. Du, *J. Rare Earths*, **28**, 219 (2010).

[10] H. Du, Y. Lan, Z. Xia, J. Sun, *Mater. Res. Bull*., **44**, 1660 (2009).

[11] L.X. Pang, H. Liu, D. Zhou, G.B. Sun, W.B. Qin, W.G. Liu, *Mater. Lett*., **72**, 128 (2012).

[12] M. Haque, D.K. Kim, *Mater. Lett*., **63**, 793 (2009).

[13] V.V. Atuchin, O.D. Chimitova, S.V. Adichtchev, J.G. Gazarov, T.A. Gavrilova, M.S. Molokeev, N.S. Surovtsev, Zh.G. Bazarova, *Mater. Lett,*. **106**, 26 (2013).

[14] L. Qin, Y. Huang, T, Tsuboi, H.J. Seo, *Mater. Res. Bull*., **47**, 4498 (2012).

[15] Y.L. Yang, X.M. Li, W.L. Feng, W.L. Li, C.Y. Tao, *J. Alloy Compd*., **505**, 239 (2010).

[16] Y. Tian, B. Chen, B. Tian, R. Hua, J. Sun, L. Cheng, H. Zhong, X. Li, J. Zhang, Y. Zheng, T. Yu, L. Huang, Q. Meng, *J. Alloy Comps*., **509**, 6096 (2011).

[17] Y. Huang, L. Zhou, Z. Tang, *Opt. Mater*., **33**, 777 (2011).

[18] Y. Tian, B. Chen, B. Tian, J. Sun, X. Li, J. Zhang, L. Cheng, H. Zhong, H. Zhong, Q. Meng, R. Hua, *Physica B*, **407**, 2556 (2012).

[19] Z. Wang, H. Liang, L. Zhou, J. Wang, M. Gong, Q. Su, *J. Lumin*., **128**, 147 (2008).

[20] Q. Chen, L. Qin, Z. Feng, R. Ge, X. Zhao, H. Xu, *J. Rare Earths*, **29**, 843 (2011).

[21] X. Shen, L. Li, F. He, X. Meng, F. Sing, *Mater. Chem. Phys*., **132**, 471 (2012).

[22] J. Zhang, X. Wang, X, Zhang, X. Zhao, X. Liu, L. *Peng, Inog. Chem. Commun*., **14**, 1723 (2011).

[23] S. Das, A.K. Mukhopadhyay, S. Datta, D. Basu, *Bull. Mater. Sci*., **32**, 1 (2009).

[24] Y. Keereeta, T. Thongtem, S. Thongtom, *Current Applied Physics*, **12,** S139 (2012).

[25] C.S. Lim, *Mater. Res. Bull*., **47**, 4220 (2012).

[26] W. Lu, L. Cheng, J. Sun, H. Zhong, X. Li, Y. Tian, J. Wan, Y. Zheng, L. Huang, T. Yu, H. Yu, B. Chen, *Physica B*, **405**, 3284 (2010).

[27] J. Sun, B. Sue, H. Du, *Infrar. Phys. Tech*., **60**, 10 (2013).

[28] Q. Sun, X. Chen, Z. Liu, F. Wang, Z. Jiang, C. Wang, *J. Alloys Comps*,. **509**, 5336 (2012).